© 2017. Published by The Company of Biologists Ltd | Journal of Experimental Biology (2017) 220, 3222-3230 doi:10.1242/jeb.162941

RESEARCH ARTICLE

Circularly polarized light detection in stomatopod crustaceans: a comparison of photoreceptors and possible function in six species

Rachel M. Templin[1,*], Martin J. How[2], Nicholas W. Roberts[2], Tsyr-Huei Chiou[3] and Justin Marshall[1]

ABSTRACT

A combination of behavioural and electrophysiological experiments have previously shown that two species of stomatopod, *Odontodactylus scyllarus* and *Gonodactylaceus falcatus*, can differentiate between left- and right-handed circularly polarized light (CPL), and between CPL and linearly polarized light (LPL). It remains unknown if these visual abilities are common across all stomatopod species, and if so, how circular polarization sensitivity may vary between and within species. A subsection of the midband, a specialized region of stomatopod eyes, contains distally placed photoreceptor cells, termed R8 (retinular cell number 8). These cells are specifically built with unidirectional microvilli and appear to be angled precisely to convert CPL into LPL. They are mostly quarter-wave retarders for human visible light (400–700 nm), as well as being ultraviolet-sensitive linear polarization detectors. The effectiveness of the R8 cells in this role is determined by their geometric and optical properties. In particular, the length and birefringence of the R8 cells are crucial for retardation efficiency. Here, our comparative studies show that most species investigated have the theoretical ability to convert CPL into LPL, such that the handedness of an incoming circular reflection or signal could be discriminated. One species, *Haptosquilla trispinosa*, shows less than quarter-wave retardance. Whilst some species are known to produce circularly polarized reflections (some *Odontodactylus* species and *G. falcatus*, for example), others do not, so a variety of functions for this ability are worth considering.

KEY WORDS: Polarization vision, Stomatopod, Circular polarization, Invertebrate vision

INTRODUCTION

Various aspects of vision are determined by environmental and behavioural need, including overall sensitivity, spatial resolution, colour sensitivity and in some species, polarization sensitivity (PS). PS is common among invertebrates (Waterman and Horch, 1966; Schwind, 1991; Labhart and Meyer, 1999), but also found in vertebrates such as fish (Hawryshyn, 1992, 2003; Coughlin and Hawryshyn, 1995; Roberts et al., 2004; Roberts and Needham, 2007). As a source of visual information and as a visual cue, the polarization of light is used by many insects for navigation (Rossel, 1993; Labhart and Meyer, 2002; Dacke, 2003; Wehner and Muller, 2006) and water body location (Schwind, 1984; Horváth and Varju, 1997). Other invertebrates such as cephalopods and crustaceans also use polarization to increase visual contrast (Temple et al., 2012; How and Marshall, 2014; How et al., 2015) and for visual signalling (Cronin et al., 2009; Marshall et al., 2014).

Polarization is a fundamental property of light and, in the context of animal vision, polarization refers to three measureable quantities for light that is made up of multiple waves (Goldstein, 2010): (1) the angle of polarization, (2) ellipticity and (3) the degree of polarization.

(1) The angle of polarization (AoP) defines the average angle at which the individual waves of light oscillate. If a linear polarizer is placed in the path of the light, then this is the angle at which the maximum intensity is transmitted.

(2) The electric fields of individual waves may be pictured as oscillating in a single plane or rotate as a circle or an ellipse around their direction of travel. Linearly polarized light (LPL) occurs when the multiple waves within a beam of light waves oscillate, on average, in a single plane. This contrasts with circularly polarized light (CPL), where the rotating individual waves result, at any one point in time, in an equal measureable intensity in all directions. Elliptically polarized light (EPL) is the most general form, in between LPL and CPL. As a numerical value, ellipticity ranges from −1 to +1 for left-handed CPL to right-handed CPL, respectively. A value in between represents EPL, and 0 is the special case for LPL.

Certain materials can change the ellipticity of polarized light according to their refractive index. The refractive index is an optical property relating to the speed that light is transmitted within a material. Some materials have more than one refractive index, which cause the components of a single wave of light to travel at different speeds. As one component lags behind the other, a phase difference is introduced. If this phase difference (or retardation) is equal to one-quarter of the light's wavelength, individual waves can be imagined to rotate in a circle around the direction of propagation, in either a clockwise or anti-clockwise direction depending on the sign of the phase delay (Hecht, 1987; Goldstein, 2010). The retardation (δ) itself depends on both the birefringence (the difference between the refractive indices of a material, Δn), the wavelength (λ) and the thickness (t) of the material, and is given by:

$$\delta(\lambda) = \frac{2\pi}{\lambda}\Delta n(\lambda)t. \quad (1)$$

An optical structure or device that creates a phase retardation of a quarter of a wavelength is called a quarter-wave retardation plate, or quarter-wave retarder. Materials that have the correct thickness and birefringence to convert LPL to CPL also work the opposite way, converting CPL to LPL.

(3) The degree of, or percentage, polarization is the ratio of the (averaged) intensity of the polarized portion of the light to its total (averaged) intensity. For LPL, this is the extent to which multiple waves oscillate at the same angle of polarization. Man-made polarizing filters generally achieve a percentage polarization close

[1]Queensland Brain Institute, University of Queensland, St Lucia, QLD 4072, Australia. [2]School of Biological Sciences, University of Bristol, Bristol BS8 1TQ, UK. [3]Department of Life Sciences, National Cheng Kung University, Tainan 701, Taiwan.

*Author for correspondence (r.templin@uq.edu.au)

R.M.T., 0000-0003-2800-5826

Received 16 May 2017; Accepted 27 June 2017

Journal of Experimental Biology

Journal of Experimental Biology (2017) 220, 3222-3230 doi:10.1242/jeb.162941

List of abbreviations

CPL circularly polarized light
CP circular polarization
EPL elliptically polarized light
LPL linearly polarized light
PS polarization sensitivity
R8 retinular cell number 8

to 100%. However, in nature, the percentage polarization of light is generally much lower. Light in the sky that scatters in the atmosphere has a maximum of around 60% (Wang et al., 2016) and can be around 40% in the ocean (Cronin et al., 2003a). Polarized animal signals can have a percentage polarization of up to 80% (Marshall et al., 2014; Jordan et al., 2016).

Sensitivity to the polarization of light relies on the intrinsic PS of the retinal photoreceptors (Roberts et al., 2011). The rhabdomeric photoreceptors of invertebrates, particularly insects and crustaceans, are polarization sensitive due to their orientational order and unidirectional microvilli (Snyder, 1973; Snyder et al., 1973; Roberts et al., 2011). Many crustaceans arrange their microvilli in two interdigitating perpendicular directions and position their photoreceptors relative to the outside world, allowing for maximal sensitivity to horizontal (H) and vertical (V) polarized light (Waterman and Horch, 1966; Alkaladi et al., 2013; Marshall and Cronin, 2014). Stomatopods, benthic marine crustaceans, have a more complex retinal structure and organization of photoreceptors (Fig. 1A,B), which enables different information channels to be utilized in parallel (Marshall et al., 1991; Marshall and Cronin, 2014). The ommatidia in the dorsal and ventral hemispheres of stomatopod eyes follow similar organization seen in other crustaceans for sensitivity to linear polarization, except that the groups of microvilli in each hemisphere are oriented at ±45 deg with respect to each other (Marshall et al., 1991) (Fig. 1C). Furthermore, stomatopods exhibit a range of eye movements including rotation and scanning, and move their eyes both independently and asymmetrically. The ability to rotate their eyes around the eye-stalk axis makes the actual angle of PS relative to the world arbitrary, potentially allowing serial analysis of polarized light (Marshall et al., 1991) or specific optimization of PS for improving contrast of an object against a background (Daly et al., 2016).

Stomatopods use both LPL and CPL visual signals for inter- and intraspecific communication. Many species broadcast a variety of different linearly polarized visual signals (Cronin et al., 2003b,c, 2009; Chiou et al., 2005). For example, the first maxillipeds of many haptosquillids are involved in sexual signals (Chiou et al., 2011) and recently, How et al. (2014) showed that the linearly polarized dimension of this signal had evolved through a mechanism of sensory bias. Circular polarization signalling may also facilitate communication (Chiou et al., 2008) and constitute a private communication channel for stomatopods, one that remains invisible to other animals, but highly salient to conspecifics (Gagnon et al., 2015). So far, however, only a few species have been found with CPL reflections and there are some species that appear to lack any polarization signal at all, potentially relying only on colour. It is worth noting there are also several potential functions other than signalling such as contrast enhancement (Daly et al., 2016) or haze reduction (Schechner et al., 2003) that might make it worthwhile evolving sensitivity to one or both types of polarized light. One of the purposes of the study described here was to begin to clarify which species have the potential sensory mechanism to detect CPL.

Stomatopod sensitivity to CPL relies on what are known as the R8 cells (retinular cell number 8) in the row 5 and 6 receptors of the midband photoreceptors (Fig. 1) (Chiou et al., 2008). The R8 cell occupies a position above the main R1–7 rhabdom and acts as a quarter-wave retarder, converting any incoming CPL to LPL. The result is that the underlying R1–7 rhabdom becomes effectively sensitive to CPL by the fact that they detect the converted LPL. What is particularly unusual about the R8 cell is that the retardation is wavelength insensitive (achromatic). Whilst Eqn 1 describes how the retardation is an inverse function of wavelength, the effective birefringence of the R8 cell increases at longer wavelengths, cancelling out the effect of the change in wavelength and creating a constant retardation (Roberts et al., 2009). This wavelength-independent effective birefringence of the R8 cell occurs through a combination of the intrinsic birefringence of the microvillar membranes and a form birefringent component owing to the ordered structure of subwavelength-sized components (Born and Wolf, 1999). The effectiveness is therefore controlled by measureable characteristics of the cell: the length of the R8 rhabdom, the diameter of the microvillar tubes and the volume packing fraction of the microvilli in the cell (Fig. 2B) (Marshall et al., 1991). Changes to either property alter the overall effective birefringence of the cell.

The reliance on cell size for a specific retardance function is itself intriguing. When comparing different species of stomatopod, differences in body size exist: adult *Haptosquilla trispinosa* are usually less than 35 mm in length compared with adult *Lysiosquillina maculata*, which can grow to more than 30 cm. Large size differences also exist developmentally within a species. For example, the post-larvae of *L. maculata* are smaller by more than a factor of 10 compared with the adults. There are concomitant differences in eye size and internal eye anatomy, and changes to eye size could limit the space available to the R8 cell both optically and anatomically (Marshall et al., 1991). Any such changes may affect the retardance and optical function of the cell, unless one factor is adjusted relative to another, and investigating these changes was a second aim of this work. We also set out to quantify the potential differences in R8 cell size across different species of stomatopod and determine what effect body size has on the cells' function as a quarter-wave retarder. Attention was paid to differences that may occur within species, such as differences between males and females, variation in size between individuals, and finally any variation within eyes according to photoreceptor placement and packing.

MATERIALS AND METHODS

Stomatopods were collected from coral reef and rubble, and mangrove areas around Lizard Island (14°40′40.8″S, 145°26′48.1″E) at a depth range of 0.5–5 m [Great Barrier Reef Marine Park Authority (GBRMPA) permit no. G12/35005.1, Fisheries Act no. 140763]. Species collected were *Gonodactylaceus falcatus*, *Gonodactylus smithii*, *Haptosquilla trispinosa* and *Lysiosquillina maculata*. Two further species, *Odontodactylus scyllarus* and *O. latirostris*, were collected from Shag Rock off North Stradbroke Island (27°25′0″S, 153°32′59.9″E) at a depth range of 10–20 m (Moreton Bay Marine Park permit no. QS2013/CVL625). The animals represent species of a wide body length range (20–200 mm) in the Gonodactyloidea and Lysiosquilloidea superfamilies. Animals were either anesthetized and dissected at the field site, or transported live to the holding aquaria at the University of Queensland, St Lucia.

Journal of Experimental Biology (2017) 220, 3222-3230 doi:10.1242/jeb.162941

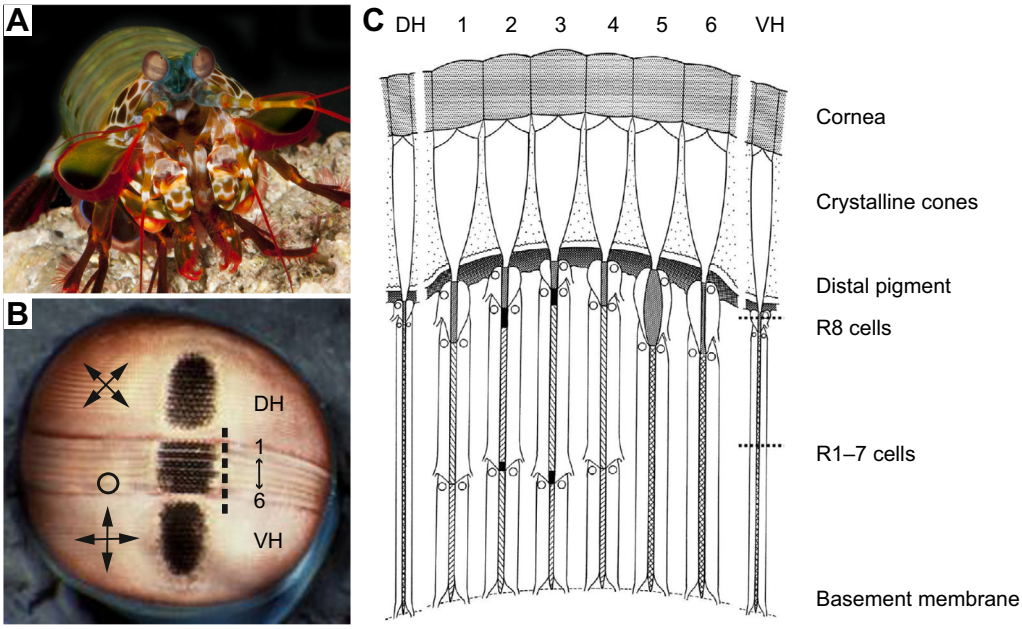

Fig. 1. Eye structure of stomatopod crustaceans. (A) *Odontodactylus scyllarus* and (B) eye showing the pseudo-pupils of the three sections, the dorsal (DH) and ventral (VH) hemispheres and the midband (showing midband rows 1 to 6). Photo credit: Roy Caldwell. The microvillar direction and resultant linear polarization of the hemispheres are represented by the crossed arrows, the circular polarization sensitivity in rows 5 and 6 by the circle. The dashed vertical line shows the area of the retina depicted in the diagrammatic section in C (Marshall et al., 1991).

Retinal cell measurements

The animals were anesthetized by cooling on ice, decapitated, and both eyes were removed and fixed in 4% paraformaldehyde and 2.5% glutaraldehyde (in PEMS buffer) (adapted from Chiou et al., 2005). Samples were post-fixed in 1% osmium tetroxide, and dehydrated in solutions with increasing ethanol concentrations. Samples were then infiltrated and embedded in EPON resin blocks for transmission electron microscopy (TEM). A microwave regime (Pelco Biowave, Ted Pella, USA) was used to aid dehydration (1 min at 150 W for each ethanol concentration) and infiltration (3 min at 150 W under vacuum).

Embedded eyes were sectioned using an ultramicrotome (EM U26, Leica, Germany). Ultrathin (~60 nm) and semithin (~500 nm) coronal sections were obtained through the entire rhabdom in rows 5 and 6 of the midband (Fig. 2). Ultrathin sections were collected on copper grids and stained with 5% uranyl acetate in 50% ethanol and Reynolds lead citrate for viewing in TEM (JEM-1010, Jeol, Japan). Semithin sections were collected on glass slides and stained with Toluidine Blue for light microscopy (Bx61, Olympus, Japan).

Images of R8 cells were collected from the high acuity region of the eye (Marshall et al., 1991), along with other regions for comparison, using both TEM and light microscopy, which allowed for measurements to be made for both the length of the R8 cell and the width of the microvilli. Light microscopy was also used to make a separate set of measurements of the length for both the R8 and the R1–7 rhabdom. The total length of the rhabdom was obtained by adding the R8 and R1–7 measurements. Measurements were acquired from TEM images using iTEM imaging software (EMSIS, Muenster, Germany). To record the length of R8 cells across the whole eye, serial sections were obtained for light microscopy through the entirety of rows 5 and 6. Images were registered in Fiji (Schindelin et al., 2012) and the positions of R8 cells were digitized using custom MATLAB-based scripts (MathWorks, Natick, MA, USA).

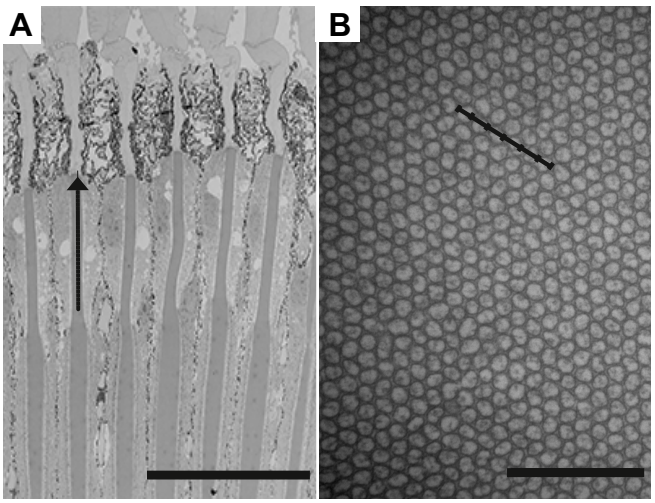

Fig. 2. R8 cell anatomy. (A) A 90 deg cross-section through the R8 cells of midband row 5; arrow indicates the length of the R8 cell. (B) A 90 deg cross-section through the tightly packed unidirectional microvilli of a row 6 R8 cell. Segmented line indicates width of 6 adjacent microvilli. Scale bars: (A) 100 µm, (B) 400 nm.

Model development and calculation of R8 retardation values

Using the methods developed by Roberts (2006) and Roberts et al. (2009), two-dimensional surface plots of retardation values were calculated based on R8 cell lengths and R8 microvilli diameter along with assumed refractive indices (Roberts et al., 2009). The surface plots allow direct visualization of the parameter sets that combine to create a specific retardation value. The contour lines depict particular values of retardance, with the bold line indicating the measurements required for quarter-wave functionality (0.25). All calculations were performed using R (version 3.2.5) and the script is available upon request. Effective dielectric tensors (Bêche and Gaviot, 2003) were calculated for microvillar diameters in the range 20–85 nm and photoreceptor lengths 40–120 µm. Onto these plots were mapped the experimentally measured values.

Statistical analysis

Data were analysed using a standardized major axis regression in R (version 3.2.5), using the smatr package, to determine the relationship between the entire rhabdom length and the length of the R1–7 and R8 rhabdoms across and between species.

Journal of Experimental Biology

Journal of Experimental Biology (2017) 220, 3222-3230 doi:10.1242/jeb.162941

RESULTS

Total rhabdom measurements

Measurements of the R1–7 and R8 rhabdoms were completed using 16 individuals from five species of stomatopod: *Gonodactylus smithii* (*n*=5), *Odontodactylus scyllarus* (*n*=2), *O. latirostris* (*n*=3), *Lysiosquillina maculata* (*n*=3) and *Haptosquilla trispinosa* (*n*=3) (Table 1, Fig. 3). Measurements of the length of the R1–7 rhabdom and the R8 rhabdom were obtained from row 5 in all individuals and in row 6 for 13 individuals. An average total rhabdom length was calculated for each individual by averaging all measurements from rows 5 and 6. For each individual between three and six measurements were made for each row.

Conservation of R8 cell length

The rhabdom length varies between individuals based on body size (Fig. 3). Larger individuals have longer rhabdom lengths than smaller individuals. R1–7 cells account for the majority of the rhabdom and the length can vary greatly both within and between species. The R8 cell, however, is more consistent in length, with only small variability between individuals of differing body lengths (Fig. 3). Plotting the total rhabdom length against the length of the R1–7 cells shows a strong correlation between variables (r=0.99), which remains strong when considering individual species (Fig. 4A). The relationship between the total rhabdom and the R8 length is weaker (r=0.54), indicating that the R8 cells are more constrained in length than the R1–7 cells (Fig. 4B). Although the slopes for individual species do vary, the relationship between the R8 cell length and the total rhabdom length remains weak in all species.

R8 measurements for use in the calculation of the retardation

To further investigate the relationship between the length of the R8 rhabdom and the width of the individual microvilli within each R8 cell (Fig. 2A,B), a second set of measurements were made from 25 individuals from six species of stomatopod: *G. smithii* (*n*=7), *G. falcatus* (*n*=3), *O. scyllarus* (*n*=3), *O. latirostris* (*n*=3), *L. maculata* (*n*=4) and *H. trispinosa* (*n*=5) (Table 2). These measurements were obtained using only light microscopy preparations where the whole length of the rhabdom could be measured. Measurements were obtained from 24 of the included individuals for row 5, and from 22 for row 6. Measurements are only included here if they were obtained for both the length of the R8 and the width of the microvilli in a single row. The number of measurements made for each individual varied (from two to 15 measurements for R8 length, and 14 to 45 measurements for microvilli width) based on the alignment of the sections through the R8. The average R8 length and microvilli width were calculated for each individual (Table 2).

Variation between species

R8 cells vary slightly in their birefringent properties between species, although for most, this has little effect on their function as quarter-wave retarders. Fig. 5 illustrates the birefringent properties of the R8 cells in each species. *Odontodactylus scyllarus*, *O. latirostris*, *L. maculata*, *G. smithii* and *G. falcatus* (Fig. 5) all have R8 cells that fall close to the line that the model predicts will provide quarter-wave retardance, resulting in a circular polarization sensitivity in rows 5 and 6. In *H. trispinosa*, the R8 cell measurements fall closer to the 0.2 line, suggesting that these cells convert CPL into EPL.

Table 1. Length measurements for the total rhabdom and R8 and R1–7 rhabdoms in five species of stomatopod

				Row 5				Row 6			
				R1–7		R8		R1–7		R8	
Species	Size (mm)	Sex	Total rhabdom (µm)	Length (µm) (s.d., *n*)	% of total	Length (µm) (s.d., *n*)	% of total	Length (µm) (s.d., *n*)	% of total	Length (µm) (s.d., *n*)	% of total
Gonodactylus smithii	19	F	375.34	291.3 (3.91, 4)	76.77	88.17 (3.69, 4)	23.23	286.75 (14.68, 6)	77.25	84.47 (4.11, 6)	22.75
	21	M	322.63	244.61 (12.71, 5)	75.82	78.02 (4.12, 5)	24.18				
	55	F	528.21	438.76 (8.58, 5)	83.07	89.45 (3.07, 5)	16.93				
	56	F	418.05	339.22 (22.22, 6)	79.63	86.76 (2.55, 6)	20.37	322.69 (2.14, 6)	78.68	87.43 (4.45, 6)	21.32
	58	M	510.69	454.66 (14.45, 5)	83.27	91.36 (4.95, 5)	16.73	384.83 (35.08, 4)	80.95	90.54 (6.43, 4)	19.05
Haptosquilla trispinosa	16	M	263.37	180.79 (4.44, 6)	70.82	74.5 (2.70, 6)	29.18	199.18 (8.76, 6)	73.37	72.28 (2.55, 6)	26.63
	25	M	269.98	203.07 (5.61, 6)	73.54	73.06 (2.07, 6)	26.46	191.73 (23.62, 6)	72.67	72.1 (2.97, 6)	27.33
	28	M	256.21	179.02 (8.37, 5)	69.81	77.42 (1.00, 5)	30.19	181.11 (6.42, 6)	70.75	74.87 (1.66, 6)	29.25
Lysiosquillina maculata	32	F	288.37	236.88 (8.48, 5)	78.76	63.9 (7.71, 5)	21.24	203.12 (14.25,5)	73.61	72.84 (3.74, 5)	26.39
	72	F	364.07	270.1 (8.33, 6)	75.75	86.46 (3.20, 6)	24.25	281.55 (14.18, 4)	75.77	90.03 (4.02, 4)	24.23
	134	F	438.34	351.89 (11.56, 3)	80.28	86.45 (2.70, 3)	19.72				
Odontodactylus latirostris	37	F	354.14	261.97 (39.25, 6)	73.54	94.25 (4.32, 6)	26.46	260.91 (17.90, 5)	74.11	91.15 (2.62, 5)	25.89
	44	F	373.13	306.06 (2.36, 5)	79.18	80.48 (3.49, 5)	20.82	273.07 (5.28, 5)	75.91	86.65 (4.37, 5)	24.09
	61	F	418.32	332.29 (2.50, 6)	77.81	94.76 (1.63, 6)	22.19	317.43 (5.27, 5)	77.5	92.16 (2.85, 5)	22.5
Odontodacyllus scyllarus	138	F	389.1	303.1 (1.57, 6)	76.91	91 (2.27, 6)	23.09	290.13 (5.09, 6)	75.54	93.96 (1.47, 6)	24.46
	167	M	451.3	365.28 (5.51, 6)	78.54	99.79 (5.82, 6)	21.46	340.52 (10.85, 6)	77.83	97.02 (2.41, 6)	22.17

M, male; F, female. Total rhabdom measurement was achieved by averaging across rows 5 and 6. Average measurements are given for each individual animal, including the percentage of total retina occupied by the R8 and R1–7 rhabdoms.

Journal of Experimental Biology (2017) 220, 3222-3230 doi:10.1242/jeb.162941

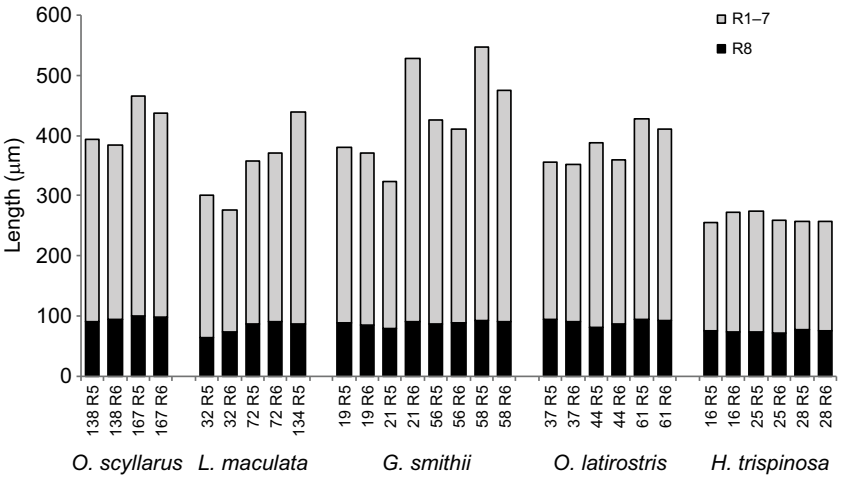

Fig. 3. Total rhabdom lengths from five species of stomatopod. The bars show the average total length of the rhabdoms of rows 5 and 6 of the acute zone of individuals from five species of stomatopod: *Odontodacyllus scyllarus* (*n*=2), *Lysiosquillina maculata* (*n*=3), *Gonodactylus smithii* (*n*=4), *Odontodactylus latirostris* (*n*=3) and *Haptosquilla trispinosa* (*n*=3). Each bar is divided into R8 (black) and R1–7 (grey). Bar labels show the individual body length (mm) and midband row, row 5 (R5) or row 6 (R6).

Variation within species

There was some variation in the size of the R8 cells, in relation to the length of the animal. This mostly affected species that displayed a large variation in body length, such as in *L. maculata* (which varied in body length from 32 to 200 mm) and in *O. scyllarus* (which varied from 45 to 167 mm). The corresponding R8 cells varied from 64.03 to 85.80 µm in *L. maculata* and from 41.87 to 95.54 µm in *O. scyllarus*, and resulted in variation in the cells' calculated birefringence (Fig. 5). Essentially, small, presumably juvenile animals in these species possess R8 cells that would not convert circular polarization to linear but to EPL, resulting in a weaker stimulation of the underlying R1–7 cells. In the case of the very small 45 mm *O. scyllarus*, this would be around half that of a perfect quarter-wave retarder.

The smaller species, such as *G. falcatus*, *G. smithii*, *H. trispinosa* and *O. latirostris*, show less variation in R8 cell measurements, while also having less variation in body length, at least for the individuals we caught. It remains possible that very small post-larval individuals in these species might display similar birefringence variation. For *G. falcatus*, *G. smithii* and *O. latirostris*, all the measurements within each species fall near the 0.25 line, indicating that they will be able to function as quarter-wave retarders. *Haptosquilla trispinosa* R8 cells fall close to the 0.2 line, suggesting either an elliptical sensitivity converting to LPL or just less efficient sensitivity to CPL, as suggested for the smaller individuals of the larger species above.

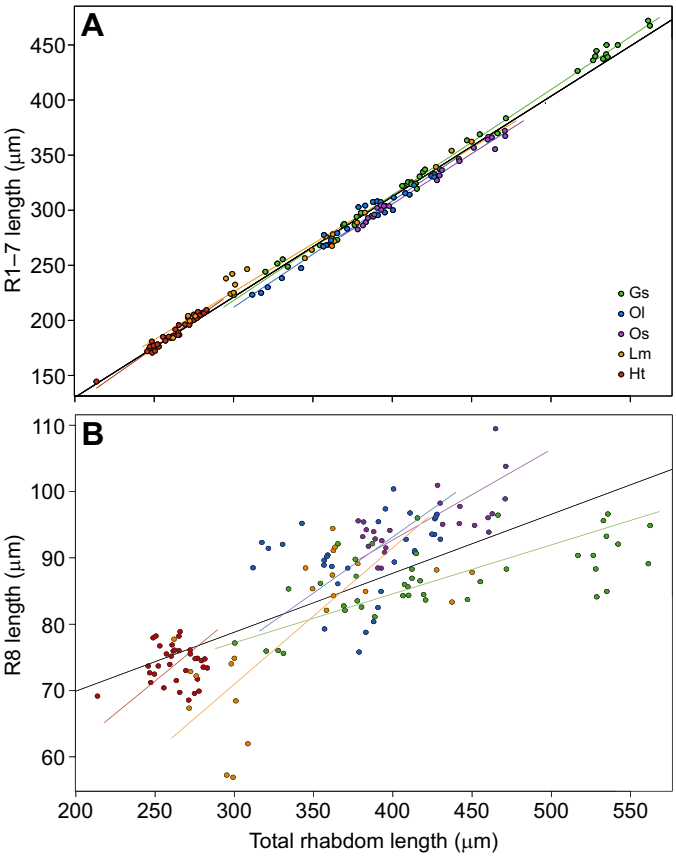

Fig. 4. Relationship of R1–7 and R8 to the total rhabdom length. (A,B) Measurements for both rows 5 and 6 from five species of stomatopod, *G. smithii* (Gs, *n*=4), *O. latirostris* (Ol, *n*=3), *O. scyllarus* (Os, *n*=2), *L. maculata* (Lm, *n*=3) and *H. trispinosa* (Ht, *n*=3). Each graph shows the slope for the overall data set (black) and one for each species. (A) Relationship of R1–7 length to total rhabdom length (overall r=0.99, Gs r=0.99, Ol r=0.97, Os r= 0.99, Lm r=0.97, Ht r=0.96). (B) Relationship of R8 length to total rhabdom length (overall r=0.54, Gs r=0.41, Ol r=0.8, Os r=0.42, Lm r=0.48, Ht r=0.002).

Variation within the retina

The properties of the R8 can also vary across the length of the midband in a single eye. To investigate the variation within the eye, measurements across the length of the midband were made in two speceis, *G. smithii* and *H. trispinosa*. The length of the R8 cells in rows 5 and 6 in *G. smithii* varied across the eye, with the cells being significantly longer in the inner part of the eye compared with the outer part (Fig. 6A). Note, however, the larger variation in R1–7 cells over this range. In *H. trispinosa*, however, the R8 cell measurements remained a more constant size in the inner and outer part of the eye (Fig. 6B). When comparing these results to the birefringent model using the microvilli width coupled with the length of the R8 cells (Fig. 7), it appears that while the R8 cells in *H. trispinosa* function similarly across the whole midband, the R8 cells in *G. smithii* vary greatly in their ability to function as quarter-wave retarders across the midband. Although the inner cells are longer than the optimal length, the outer cells are too short, and it is cells in and around the acute zone that have R8 cells that fall within the correct size range for good quarter-wave retardance.

DISCUSSION

The results of this study illustrate that, while there are several sources of variability in the size and thus the birefringence of the R8

Journal of Experimental Biology (2017) 220, 3222-3230 doi:10.1242/jeb.162941

Table 2. Summary of the R8 measurements obtained from each animal

			Row 5		Row 6	
Species	Size (mm)	Sex	R8 length (μm) (s.d., *n*)	Microvilli width (nm) (s.d., *n*)	R8 length (μm) (s.d., *n*)	Microvilli width (nm) (s.d., *n*)
Gonodactylus smithii	19	F	85.54 (4.18, 6)	59.68 (7.08, 15)	83.94 (3.45, 6)	57.43 (5.72, 14)
	55	F	86.60 (3.04, 5)	57.42 (5.85, 18)	87.17 (6.08,3)	60.72 (7.01, 38)
	49	F	87.23 (3.48, 14)	57.71 (7.53, 26)		
	58	M	88.51 (2.02, 12)	52.11 (4.20, 16)	91.14 (4.14, 6)	58.96 (4.31, 23)
	56	F	82.63 (2.04, 15)	51.65 (5.71, 25)	83.47 (1.57, 12)	52.70 (4.05, 26)
	21	M	78.02 (4.12, 5)	54.56 (5.87, 25)		
	68	M	77.51 (2.80, 12)	54.14 (4.08, 17)	75.25 (3.49, 7)	61.39 (4.20, 17)
Gonodactylaceus falcatus	38	M	74.75 (3.41, 15)	46.40 (5.40, 34)	63.42 (3.17, 4)	48.86 (4.89, 17)
	23	M	79.84 (2.52, 6)	45.28 (4.10, 35)	81.36 (1.15, 5)	55.5 (5.64, 27)
	44	M	80.37 (3.39, 10)	45.62 (2.09, 20)	79.78 (1.98, 5)	59.76 (5.27, 14)
Odontodacyllus syllarus	45	M	41.87 (2.29, 4)	44.66 (3.45, 8)		
	138	F	91.35 (4.74, 11)	56.38 (7.15, 32)	89.24 (7.67, 6)	59.01 (8.34, 44)
	167	M	95.54 (3.73, 12)	56.31 (7.02, 25)	92.31 (3.01, 16)	74.59 (7.25, 25)
Odontodactylus latirostris	61	F	92.11 (1.70, 10)	64.75 (5.78, 34)	92.93 (2.20, 4)	63.78 (7.32, 32)
	44	F	78.15 (2.53, 7)	61.71 (7.45, 45)	86.06 (3.62, 5)	69.95 (8.36, 37)
	37	F	97.97 (3.65, 18)	71.33 (8.18, 24)	90.22 (3.10, 4)	63.38 (5.52, 28)
Lysiosquillina maculata	134	F	82.23 (3.27, 5)	56.95 (9.26, 18)	81.15 (1.58, 4)	81.47 (10.33, 14)
	72	F	84.60 (4.62, 6)	54.11 (7.23, 19)	84.11 (3.37, 4)	58.19 (6.78, 20)
	32	F	64.03 (7.98, 5)	56.09 (3.58, 15)	65.70 (3.90, 9)	73.05 (10.61, 15)
	200	M	85.8 (4.33, 2)	59.84 (3.12, 25)	79.67 (N/A, 1)	56.53 (3.40, 25)
Haptosquilla trispinosa	16	M	72.21 (5.38, 19)	57.22 (5.75, 31)	66.49 (4.83, 10)	59.76 (6.56, 34)
	16	M	68.88 (1.65, 12)	56.59 (5.19, 41)	68.21 (4.22, 5)	61.08 (7.93, 28)
	25	M	73.31 (2.64, 11)	55.16 (7.29, 25)	71.37 (1.89, 15)	55.98 (6.84, 31)
	28	M	65.73 (13.78, 11)	47.37 (3.45, 25)	74.07 (3.63, 13)	58.95 (7.22, 33)
	21	F			63.61 (4.74, 7)	48.04 (4.71, 30)

M, male; F, female. Average length of the R8 and width of the microvilli for both rows 5 and 6 are given.

cells across stomatopod species, R8 cells appear more conserved than other cells in the retina. This suggests adaptive pressure for R8 cells to stay within a certain size range to maintain the ability to act as quarter-wave retarders. There is a strong relationship between the length of the R1–7 cells and total rhabdom length, but less of a correlation between the R8 length and the total rhabdom length. This relationship highlights that the R8 length is conserved when the total size of the rhabdom increases.

Interspecies variability

Despite investigating several species of stomatopods with a large range of body sizes, habitat preferences and ecological constraints, the size of the R8 cells remained largely similar. As noted, this suggests significant adaptive pressure to keep these cell types within a functional size range for quarter-wave retardance. The exception to this is *H. trispinosa*, where the R8 cells' retardance suggests sensitivity to an elliptical form of polarized light with retardance closer to 0.2 than 0.25. Why *H. trispinosa* would be tuned to detect elliptical polarized light (EPL) is not yet known, but it is fascinating to speculate that its eye may be tuned more specifically to a particular ellipticity in the environment. Alternatively, selection for precise quarter-wave retardance in this species may be relaxed, as CPL is less significant for its current survival needs. Notably, this species does display strong linear polarization signals (Cronin et al., 2009).

Body size

Within a species, most cells perform well as quarter-wave retarders, but there was some individual variability, particularly where the total body size of the animals varied greatly from juvenile to adult, such as *L. maculata* and *O. scyllarus*. This indicates that, while large individuals of a species detect CPL, small individuals of the same species, perhaps not yet sexually mature and with no need to pay attention to circular polarization, may not. In these cases, instead of opting for a shorter R1–7 rhabdom, the birefringent function of the R8 cell is compromised, suggesting that a critical R1–7 length is required for the rhabdom to maintain sensitivity. Additionally, once the R8 has reached the point of quarter-wave retardance it no longer continues to increase in size, i.e. the R8 seems to stop increasing in size at sensitivity to circularly polarized light, allowing large relative increases in the R1–7 rhabdom.

Sensitivity changes within the eye

Investigation of R8 sizes across the midband in *H. trispinosa* and *G. smithii* provided evidence that R8 cell length can also vary within an individual eye. While the length of the R8 cells in *H. trispinosa* displayed a similar size across the midband, *G. smithii* displays more variability in R8 cell length, with the inner, more forward-facing part of the midband having longer R8 cells than the outer, lateral part. In fact, *G. smithii* only have circular polarization sensitivity in the central part of the midband, in ommatidia around the acute zone. It may be that the elongate design of this eye places spatial limits on the ommatidial dimensions and that retaining good CPL sensitivity in the forward-facing zones is enough. The eye of *H. trispinosa* is evenly spherical along the midband direction (as are the eyes of all other species examined; Marshall et al., 1991; Marshall and Land, 1993), making it possible to retain the same R8 dimensions along the whole midband, including the acute zone, without compromising the size of the R1–7.

Function of circular polarization vision

Previous behavioural tests have shown that *O. scyllarus* can learn left from right circular polarization in feeding trials (Chiou et al., 2008). It is also known that *G. falcatus* prefers not to enter burrows emitting CPL (Gagnon et al., 2015), although the actual use of CPL in either of these species or others included in this study is still hypothetical. It is not known, for instance, if food items of *O.*

Journal of Experimental Biology (2017) 220, 3222-3230 doi:10.1242/jeb.162941

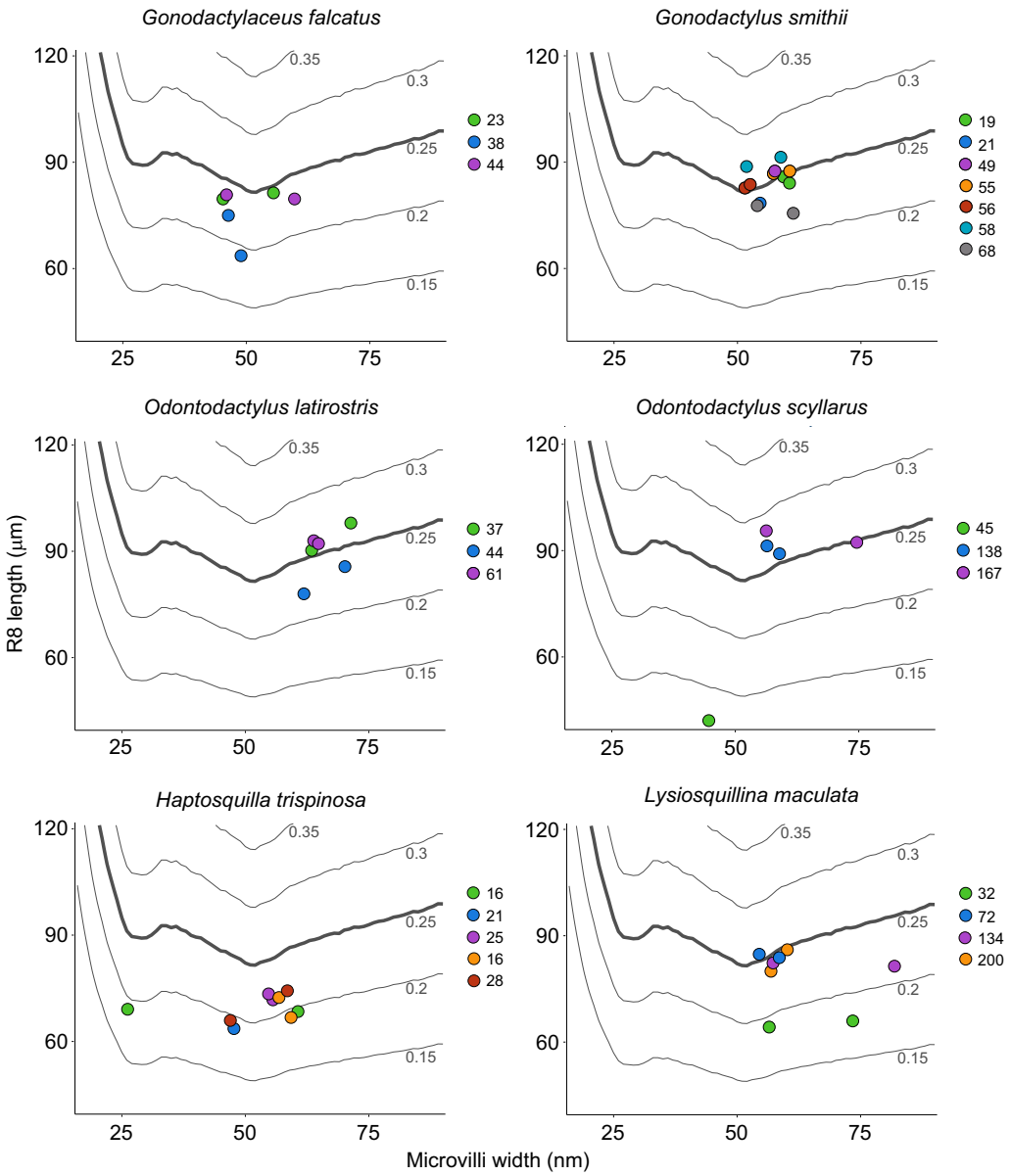

Fig. 5. Birefringent properties of R8 cells from different species of stomatopod. Measurements for the R8 cells combined with the calculations of retardation values to predict the birefringence in different species *G. falcatus* (*n*=3), *G. smithii* (*n*=7), *O. latirostris* (*n*=3), *O. scyllarus* (*n*=3), *H. trispinosa* (*n*=5) and *L. maculata* (*n*=4). Contour lines represent modelled retardance values for corresponding R8 cell length and microvillus widths. Bold contour lines represent the value for quarter-wave retardance (0.25). Each point is the average of measurements (R8 length and microvillus length) for either row 5 or row 6 with different individuals shown in different colours [individual body length (in mm) is given in the associated key for each panel].

scyllarus reflect CPL differentially, or if this species just manages to transfer its ability for discrimination to an isolated feeding circumstance in behavioural trials. *Odontodactylus* species and specifically *G. falcatus* are known to reflect CPL (Chiou et al., 2008; Gagnon et al., 2015) and one possible function is inter- or intraspecific signalling. However, this is yet to be directly tested. In the context of other animals, scarab beetles have been known for many years to reflect CPL (Michelson, 1911) and initial behaviour evidence suggested sensitivity to CPL in American jewel beetles (Brady and Cummings, 2010). However, this sensitivity was not found in a more recently conducted survey of four related European species (Blahó et al., 2012). If CP is used by stomatopods for inter- or intraspecific signalling, it should be noted that so far only *Odontodactylus cultrifer*, *G. falcatus*, *Squilla mantis* and some *Neogonodactylus* species are known to exhibit strongly polarized CP reflections (Chiou et al., 2008; Gagnon et al., 2015), but further investigation is underway to quantify polarized signals more thoroughly in other species.

LPL-insensitive detection channels

Finally, it is worth considering that the R8 cells in rows 5 and 6 of the midband may not have originally evolved with the primary purpose of converting CPL to LPL. The R8 cells in rows 5 and 6 are sensitive to ultraviolet wavelengths of light because the R8 of row 5 is orientated perpendicular to the R8 of row 6, and by comparison they act as an ultraviolet PS channel (Kleinlogel and Marshall, 2009) in the midband sensitive to LPL. However, if the R1–7 photoreceptors below are primarily concerned with colour vision or a measure of intensity (Marshall et al., 1991; Thoen et al., 2014), then elimination of PS is ideal and allows them to potentially be

Journal of Experimental Biology (2017) 220, 3222-3230 doi:10.1242/jeb.162941

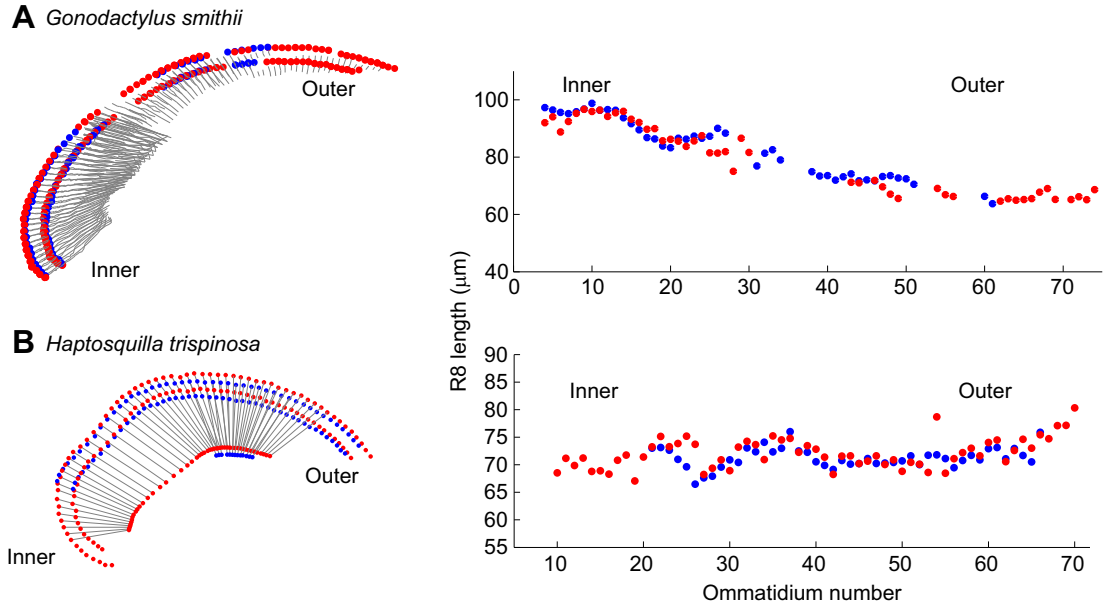

Fig. 6. R8 length across the whole midband. Reconstruction of the proximal and distal positions of R8 cells from row 5 (blue) and row 6 (red) across the length of the midband (from the inner to the outer part of the eye) in *G. smithii* (A) and *H. trispinosa* (B). Left: three-dimensional reconstruction of distal and proximal positions of the R8 cell (and, in some cases, the main rhabdom). Right: R8 length of each ommatidial unit across the whole midband.

subject to false colours (Kelber et al., 2001) or false signals. Other arthropods avoid sensitivity to LPL by (1) producing rhabdomeres with microvilli that are misaligned, (2) forming twisted rhabdomeres with microvilli of low birefringence or (3) summing (in the lamina) the signals of receptors with mutually perpendicular microvilli (Eguchi and Waterman, 1967, 1973; Waterman, 1981; Marshall et al., 1991). The use of the R8 cell as a quarter-wave retarder provides a novel approach to remove the linear polarization information in the signal. Interestingly, this way of removing unwanted LPL is also used in photography, where CPL rather than LPL filters are used (Goldberg, 1992). A clear, although again hypothetical, evolutionary progression could therefore drive a quarter-wave retarder to be exploited through the emergence of CPL signals to provide certain species with the sensory ability to detect CPL.

While several alternative, and not necessarily mutually exclusive, hypotheses exist for the evolution of this apparently complex polarization vision system, it is worth re-iterating that our knowledge of what the stomatopods actually do with polarization vision and polarized reflections, where they exist, is still in its infancy. Field observations and behavioural analyses would help place such hypotheses on a firm foundation of reality.

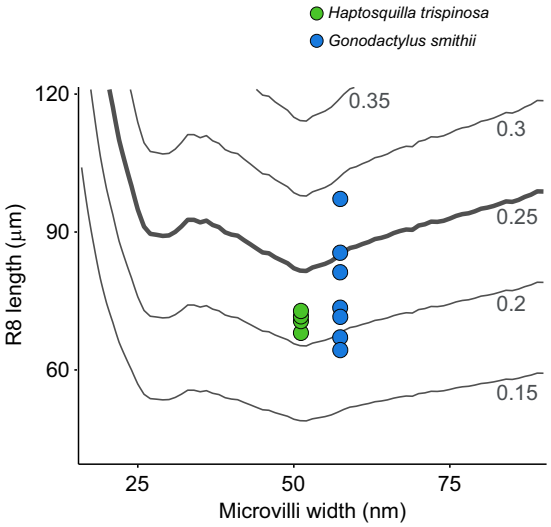

Fig. 7. Birefringent properties modelled across the whole midband of *H. trispinosa* and *G. smithii*. R8 length obtained from measurements across the whole midband of *H. trispinosa* and *G. smithii* were coupled with the average microvilli width for each species. Seven points are plotted for each species. The consistency in the size of R8 cells in *H. trispinosa* results in many points lying on top of one another. In contrast, the R8 cells of *G. smithii* vary greatly in function across the midband, altering their birefringent ability and consequently their ability to function as quarter-wave retarders.

Acknowledgements
The authors wish to acknowledge the facilities, and the scientific and technical assistance, of the Australian Microscopy and Micro analysis Research Facility at the Centre for Microscopy and Microanalysis, The University of Queensland, and Dr Hanne Thoen for her comments on the manuscript.

Competing interests
The authors declare no competing or financial interests.

Author contributions
Conceptualization: R.M.T., M.J.H., N.W.R., T.-H.C., J.M.; Methodology: R.M.T., M.J.H., N.W.R., T.-H.C.; Software: N.W.R.; Formal analysis: R.M.T., M.J.H., N.W.R.; Investigation: R.M.T., M.J.H.; Writing - original draft: R.M.T., N.W.R.; Writing - review & editing: R.M.T., M.J.H., N.W.R., T.-H.C., J.M.; Supervision: J.M.; Funding acquisition: N.W.R., J.M.

Funding
This work was supported by grants awarded to J.M. by the Asian Office of Aerospace Research and Development (AOARD-12-4063) and the Australian Research Council (FL140100197), and to N.W.R. by Air Force Office of Scientific Research (AFOSR FA8655-12-2112).

References

Alkaladi, A., How, M. J. and Zeil, J. (2013). Systematic variations in microvilli banding patterns along fiddler crab rhabdoms. *J. Comp. Physiol. A Neuroethol. Sens. Neural Behav. Physiol.* **199**, 99-113.

Bêche, B. and Gaviot, E. (2003). Matrix formalism to enhance the concept of effective dielectric constant. *Optics Commun.* **219**, 15-19.

Blahó, M., Egri, Á., Hegedüs, R., Jósvai, J., Tóth, M., Kertész, K., Biró, L. P., Kriska, G. and Horváth, G. (2012). No evidence for behavioral responses to

circularly polarized light in four scarab beetle species with circularly polarizing exocuticle. *Physiol. Behav.* **105**, 1067-1075.
Born, M. and Wolf, E. (1999). *The Principles of Optics*. Cambridge: Cambridge University Press.
Brady, P. and Cummings, M. (2010). Differential response to circularly polarized light by the jewel scarab beetle *Chrysina gloriosa*. *Am. Nat.* **175**, 614-620.
Chiou, T.-H., Cronin, T. W., Caldwell, R. L. and Marshall, J. (2005). Biological polarized light reflectors in stomatopod crustaceans. **5888**, 58881B-58881B-9.
Chiou, T.-H., Kleinlogel, S., Cronin, T., Caldwell, R., Loeffler, B., Siddiqi, A., Goldizen, A. and Marshall, J. (2008). Circular polarization vision in a stomatopod crustacean. *Curr. Biol.* **18**, 429-434.
Chiou, T.-H., Marshall, N. J., Caldwell, R. L. and Cronin, T. W. (2011). Changes in light-reflecting properties of signalling appendages alter mate choice behaviour in a stomatopod crustacean *Haptosquilla trispinosa*. *Mar. Freshw. Behav. Physiol.* **44**, 1-11.
Coughlin, D. J. and Hawryshyn, C. W. (1995). A cellular basis for polarized-light vision in rainbow trout. *J. Comp. Physiol. A* **176**, 261-272.
Cronin, T. W., Shashar, N., Caldwell, R. L., Marshall, J., Cheroske, A. G. and Chiou, T. H. (2003a). Polarization signals in the marine environment. In *Polarization Science and Remote Sensing* (ed. J. A. Shaw and J. S. Tyo), pp. 85-92. Bellingham: Spie-Int Soc Optical Engineering.
Cronin, T. W., Shashar, N., Caldwell, R. L., Marshall, J., Cheroske, A. G. and Chiou, T. H. (2003b). Polarization vision and its role in biological signalling. *Integr. Comp. Biol.* **43**, 549-558.
Cronin, T. W., Shashar, N., Caldwell, R. L., Marshall, J. N., Cheroske, A. G. and Chiou, T.-H. (2003c). Polarization signals in the marine environment. *Proc. SPIE* **5158**, 85-92.
Cronin, T. W., Chiou, T.-H., Caldwell, R. L., Roberts, N. and Marshall, J. (2009). Polarization signals in mantis shrimps. *Proc. SPIE* 7461, 74610C-74610C-10.
Dacke, M. (2003). Twilight orientation to polarised light in the crepuscular dung beetle *Scarabaeus zambesianus*. *J. Exp. Biol.* **206**, 1535-1543.
Daly, I. M., How, M. J., Partridge, J. C., Temple, S. E., Marshall, N. J., Cronin, T. W. and Roberts, N. W. (2016). Dynamic polarization vision in mantis shrimps. *Nat. Commun.* **7**, 12140.
Eguchi, E. and Waterman, T. H. (1967). Cellular basis for polarized light perception in the spider crab, *Libinia*. *Z. Zellforsch. Mikrosk. Anat.* **84**, 87-101.
Eguchi, E. and Waterman, T. H. (1973). Orthogonal microvillus pattern in the eighth rhabdomere of the rock crab *Grapsus*. *Z. Zellforsch.* **137**, 145-157.
Gagnon, Y. L., Templin, R. M., How, M. J. and Marshall, N. J. (2015). Circularly polarized light as a communication signal in mantis shrimps. *Curr. Biol.* **25**, 3074-3078.
Goldberg, N. (1992). *Camera Technology: The Dark Side of the Lens*. Cambridge, MA: Academic Press.
Goldstein, D. (2010). *Introduction to Polarized Light. Polarized Light*, 3rd edn. Boca Raton, FL: CRC Press.
Hawryshyn, C. W. (1992). Polarisation vision in fish. *Am. Sci.* **80**, 164-175.
Hawryshyn, C. W. (2003). Mechanisms of ultraviolet polarization vision in fishes. In *Sensory Processing in Aquatic Environments* (ed. S. P. Collin and N. J. Marshall), pp. 252-265. New York: Springer.
Hecht, E. (1987). *Optics*. Boston, MA: Addison Wesley.
Horváth, G. and Varju, D. (1997). Polarization patter of freshwater habitats recorded by video polarimetry in red, green and blue spectral ranges and its relevance for water detection by aquatic insects. *J. Exp. Biol.* **200**, 1155-1163.
How, M. J. and Marshall, N. J. (2014). Polarization distance: a framework for modelling object detection by polarization vision systems. *Proc. Biol. Sci.* **281**, 20131632.
How, M. J., Porter, M. L., Radford, A. N., Feller, K. D., Temple, S. E., Caldwell, R. L., Marshall, N. J., Cronin, T. W. and Roberts, N. W. (2014). Out of the blue: the evolution of horizontally polarized signals in Haptosquilla (Crustacea, Stomatopoda, Protosquillidae). *J. Exp. Biol.* **217**, 3425-3431.
How, M. J., Christy, J. H., Temple, S. E., Hemmi, J. M., Marshall, N. J. and Roberts, N. W. (2015). Target detection is enhanced by polarization vision in a fiddler crab. *Curr. Biol.* **25**, 3069-3073.
Jordan, T. M., Wilby, D., Chiou, T.-H., Feller, K. D., Caldwell, R. L., Cronin, T. W. and Roberts, N. W. (2016). A shape-anisotropic reflective polarizer in a stomatopod crustacean. *Sci. Rep.* **6**, 21744.
Kelber, A., Thunell, C. and Arikawa, K. (2001). Polarisation-dependent colour vision in *Papilio* butterflies. *J. Exp. Biol.* **204**, 2469-2480.
Kleinlogel, S. and Marshall, N. J. (2009). Ultraviolet polarisation sensitivity in the stomatopod crustacean *Odontodactylus scyllarus*. *J. Comp. Physiol. A Neuroethol. Sens. Neural Behav. Physiol.* **195**, 1153-1162.
Labhart, T. and Meyer, E. P. (1999). Detectors for polarized skylight in insects: a survey of ommatidial specializations in the dorsal rim area of the compound eye. *Microsc. Res. Tech.* **47**, 368-379.
Labhart, T. and Meyer, E. P. (2002). Neural mechanisms in insect navigation: polarization compass and odometer. *Curr. Opin. Neurobiol.* **12**, 707-714.
Marshall, J. and Land, M. F. (1993). Some optical features of the eyes of stomatopods. II. Ommatidial design, sensitivity and habitat. *J. Comp. Physiol. A* **173**, 583-594.
Marshall, J. N. and Cronin, T. W. (2014). *Crustacean Polarization vision. Polarized Light and Polarization Vision in Animal Sciences*. New York: Springer.
Marshall, N. J., Land, M. F., King, C. A. and Cronin, T. W. (1991). The compound eyes of mantis shrimps (Crustacea, Hoplocarida, Stomatopoda). I. Compound eye structure: the detection of polarized light. *Philos. Trans. R. Soc. Lond. B Biol. Sci.* **334**, 33-56.
Marshall, N. J., Roberts, N. W. and Cronin, T. W. (2014). *Polarization Signals. Polarized Light and Polarization Vision in Animal Science*. Berlin: Springer.
Michelson, A. A. (1911). LXI. On metallic colouring in birds and insects. *Philos. Magazine Ser. 6* **21**, 554-567.
Roberts, N. W. (2006). The optics of vertebrate photoreceptors: anisotropy and form birefringence. *Vision Res.* **46**, 3259-3266.
Roberts, N. W. and Needham, M. G. (2007). A mechanism of polarized light sensitivity in cone photoreceptors of the goldfish *Carassius auratus*. *Biophys. J.* **93**, 3241-3248.
Roberts, N. W., Gleeson, H. F., Temple, S. E., Haimberger, T. J. and Hawryshyn, C. W. (2004). Differences in the optical properties of vertebrate photoreceptor classes leading to axial polarization sensitivity. *J. Opt. Soc. Am. A* **21**, 335-345.
Roberts, N. W., Chiou, T.-H., Marshall, N. J. and Cronin, T. W. (2009). A biological quarter-wave retarder with excellent achromaticity in the visible wavelength region. *Nat. Photonics* **3**, 641-644.
Roberts, N. W., Porter, M. L. and Cronin, T. W. (2011). The molecular basis of mechanisms underlying polarization vision. *Philos. Trans. R. Soc. Lond. B Biol. Sci.* **366**, 627-637.
Rossel, S. (1993). Navigation by bees using polarised skylight. *Comp. Biochem. Physiol.* **104A**, 965-708.
Schechner, Y. Y., Narasimhan, S. G. and Nayar, S. K. (2003). Polarization-based vision Through Haze. *Appl. Opt.* **42**, 511-525.
Schindelin, J., Arganda-Carreras, I., Frise, E., Kaynig, V., Longair, M., Pietzsch, T., Preibisch, S., Rueden, C., Saalfeld, S., Schmid, B. et al. (2012). Fiji: an open-source platform for biological-image analysis. *Nat. Methods* **9**, 676-682.
Schwind, R. (1984). Evidence for true polarization vision based on a two-channel analyzer system in the eye of the water bug, *Notonecta glauca*. *J. Comp. Physiol. A* **154**, 53-57.
Schwind, R. (1991). Polarization vision in water insects and insects living on a moist substrate. *J. Comp. Physiol. A* **169**, 531-540.
Snyder, A. W. (1973). Polarization sensitivity of individual retinula cells. *J. Comp. Physiol. A* **83**, 331-360.
Snyder, A. W., Menzel, R. and Laughlin, S. B. (1973). Structure and function of the fused rhabdom. *J. Comp. Physiol. A* **87**, 99-135.
Temple, S. E., Pignatelli, V., Cook, T., How, M. J., Chiou, T.-H., Roberts, N. W. and Marshall, N. J. (2012). High-resolution polarisation vision in a cuttlefish. *Curr. Biol.* **22**, R121-R122.
Thoen, H. H., How, M. J., Chiou, T. H. and Marshall, J. (2014). A different form of color vision in mantis shrimp. *Science* **343**, 411–413.
Wang, X., Gao, J., Fan, Z. and Roberts, N. W. (2016). An analytical model for the celestial distribution of polarized light, accounting for polarization singularities, wavelength and atmospheric turbidity. *J. Opt.* **18**, 065601.
Waterman, T. H. (1981). Polarisation sensitivity. In *Handbook of Sensory Physiology*, Vol. VII/6B (ed. H. Autrum), pp. 281-471. Berlin: Springer-Verlag.
Waterman, T. H. and Horch, K. W. (1966). Mechanism of polarized light perception. *Science* **154**, 467-475.
Wehner, R. and Muller, M. (2006). The significance of direct sunlight and polarized skylight in the ant's celestial system of navigation. *Proc. Natl. Acad. Sci. USA* **103**, 12575-12579.